Zeitschrift: Helvetica Physica Acta
Band: 56 (1983)
Heft: 1-3

Artikel: Point-contact spectroscopy
Autor: Jansen, A.G.M. / Gelder, A.P. van / Duif, A.M.
DOI: https://doi.org/10.5169/seals-115370

Helvetica Physica Acta,
Vol. 56 (1983) 209-222

0018-0238/83/010209-14$1.50+0.20/0

POINT-CONTACT SPECTROSCOPY

A.G.M. Jansen, A.P. van Gelder, A.M. Duif, P. Wyder and N. d'Ambrumenil*

Research Institute for Materials, University of Nijmegen, Toernooiveld,
6525 ED Nijmegen, The Netherlands.

Abstract. Point contacts between metals show deviations from Ohm's law, which are used for a spectroscopic analysis of the scattering of electrons in a metal. A theoretical model is presented for the electrical transport problem of a metallic constriction, based on the solution of the Boltzmann equation. Experiments demonstrate that the electron-phonon interaction function α^2F can be measured directly in normal metals. Other scattering mechanisms than the electron-phonon interaction can also be detected with point contacts. Examples are given for dilute alloys of metals with paramagnetic impurities.

Introduction

In the simple Drude model for the electrical conduction in a metal the electrons are accelerated by the electric field yielding a drift velocity for the electronic system. In the limit of small fields the scattering of the electrons in a metal is independent of the gain in energy of the electrons between subsequent collisions. The drift velocity is proportional to the electric field and it follows that the current density is proportional to the electric field; this is known as Ohm's law. The conductivity in a metal is high and therefore the small field limit is appropriate for a description of the electrical conduction in a bulk metal. However, in metallic point contacts with dimensions smaller than the electric mean free path the situation is quite different. By an applied electric field the electrons are accelerated within a mean free path by passing the contact region and the scattering processes depend on the energy of the accelerated electrons. For such a metallic constriction the relation between current and voltage is not linear. The observed deviations from Ohm's law contain spectroscopic information about the scattering of electrons in a metal. The spectroscopic method, which deals with these interesting non-linear phenomena in the electrical resistance of point contacts, is called point-contact spectroscopy.

In the development of point-contact spectroscopy to a useful experimental technique the first and most important discovery was done by Yanson[1]. He

examined the current-voltage characteristics of tunnel junctions with a short-circuit between the metal films and found remarkable deviations from Ohm's law. The contact resistance increased at applied voltages corresponding to the energies of the phonons of the metal which formed the junction. The fascinating result of Yanson's investigations was that the measured second derivative of the voltage V with respect to the current I gives as a function of the applied voltage a direct determination of the energy-dependence of the function α^2F for the electron-phonon interaction. The function α^2F is an average over the Fermi surface of the phonon density of states F multiplied with the squared matrix element for the electron-phonon interaction. The spectra of the phonon density of states have been studied most extensively by neutron scattering and superconducting tunneling, which experimental techniques yield respectively the functions F and α^2F. Especially for normal metals the point-contact method is of great interest because for the first time the spectral distribution of the electron-phonon interaction could be measured directly.

The experimental technique got a much wider application by the use of pressure-type point contacts[2]. The spear-anvil technique for the preparation of a constriction allowed to study samples in an easier way and more materials (even single crystals) could be studied with point-contact spectroscopy.

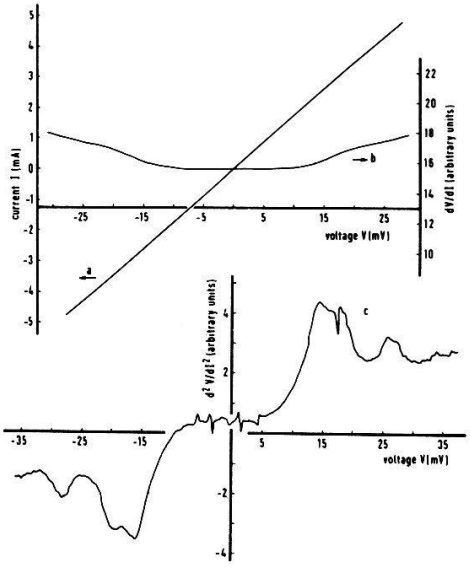

In Figure 1 we give an example of the recorder output of the I-V, dV/dI and d^2V/dI^2 curves as measured for a copper spear-anvil contact immerged in liquid helium. In the second derivative d^2V/dI^2 the structure around 17 and 28 mV

Figure 1. Direct recorder output of the I-V, dV/dI-V and d^2V/dI^2-V curves for a Cu point contact. Resistance R = 5.7 Ω and temperature T = 1.2 K.

coincides with the two transverse and single longitudinal modes in copper.

In this paper we will first treat the problem of a contact resistance in the Knudsen regime, where the electronic mean free path is large compared to the contact diameter. The theoretical background for an explanation of the observed non-linear phenomena will be given, applied to the electron-phonon interaction. It can easily be shown how the spectroscopic method applies to any arbitrary scattering mechanism. Experimental results will be presented for the electron-phonon interaction in normal metals. Other applications will be mentioned, more specifically to Kondo systems and spin glasses.

Resistance of a constriction

At the beginning of this century Maxwell[3] solved the problem of the resistance for a metallic contact. Starting with Poisson's equation and using Ohm's law Maxwell derived the contours of constant potential and calculated for a circular orifice with radius a the resistance

$$R_M = \rho/2a \ , \qquad (1)$$

where ρ is the bulk resistivity of the metal. Obviously, the Maxwell resistance resembles the resistance of a sample with length a and cross-section a^2. Maxwell's expression for the contact resistance is correct in the regime, where the contact dimension a is large compared to the mean free path ℓ of the electrons. Sharvin[4] realized that the transport of electrons is no longer diffuse for contacts with $\ell/a \gg 1$, but ballistic. In the limit of clean contacts the expression for the resistance R_{Sh} is given by[4]

$$R_{Sh} = 4\rho\ell/3A \qquad (2)$$

for a constriction with contact area A. The Sharvin resistance is independent of the mean free path. To relax the condition $\ell/a \gg 1$ an expansion can be made with respect to the inverse Knudsen number a/ℓ for the contact resistance:

$$R \sim R_{Sh} \ (1 + a/\ell) \ . \qquad (3)$$

In the two limiting regimes ($\ell \gg a$, $\ell \ll a$) formula (3) reduces respectively to the Sharvin and Maxwell resistance. For the case that the mean free path depends on the applied voltage we have $R(V) \propto 1/\ell(V)$. Equation (3) is the most important formula for the interpretation of point-contact spectra. A measurement of the resistance of a point contact as a function of the applied voltage gives a direct determination of the inelastic scattering rate of the conduction electrons.

The Boltzmann equation

In the previous paragraph we have given some arguments for an intuitive understanding of the point-contact method. For a more accurate evaluation the full non-linear Boltzmann equation for this transport problem has to be solved. These theories now exist[5,6,7] and we will give a brief summary of the essential results.

In terms of the electron distribution-function $f(\underline{r},\underline{k})$ the current through an orifice is given by the following integral over the contact area (situated in the $z = 0$ plane)

$$I = 2e \int_{\text{orifice}} \underline{d^2 r} \sum_{\underline{k}} v_{\underline{k}z} \, f(\underline{r},\underline{k}) \ , \tag{4}$$

where $v_{\underline{k}}$ is the velocity of an electron with wavevector $\underline{k}$. The distribution function $f(\underline{r},\underline{k})$ is found as a solution of the Boltzmann equation

$$\underline{v}_{\underline{k}} . \underline{\nabla}_{\underline{r}} \, f(\underline{r},\underline{k}) + \frac{e}{\hbar} \underline{E} . \underline{\nabla}_{\underline{k}} \, f(\underline{r},\underline{k}) = \left. \frac{\partial f}{\partial t} \right|_{\text{coll.}} \ . \tag{5}$$

The term at the right-hand side contains all relevant collisions of the electrons. Far from the contact region the boundary conditions for the potential ϕ and the distribution function $f(\underline{r},\underline{k})$ are

$$\begin{aligned} &\phi(z \to \pm \infty) \quad = \pm \, eV/2 \\ &\text{and} \quad f(z \to \pm \infty, \underline{k}) = f_o(\varepsilon_{\underline{k}}) \ , \end{aligned} \tag{6}$$

where $f_o(\varepsilon_{\underline{k}})$ is the usual Fermi-Dirac distribution for equilibrium. Self-consistently the potential $\phi(\underline{r})$ can be determined from the argument that no extra charge may be introduced by the choice of the distribution $f(\underline{r},\underline{k})$. Charge neutrality gives

$$e \sum_{\underline{k}} [\, f(\underline{r},\underline{k}) - f_o(\varepsilon_{\underline{k}}) \,] = 0 \ . \tag{7}$$

The solution of the Boltzmann equation goes via iteration, with $f = f^{(0)} + f^{(1)} + \ldots$. The zeroth order term of the contribution to the distribution function describes the field emission of electrons in the absence of scattering and yields the Sharvin current. The next terms are due to scattering processes (single, double collisions). The first order term $f^{(1)}$ in the iteration gives a negative contribution to the current: accelerated electrons are scattered back through the orifice. For the solution of the Boltzmann equation Chamber's method of path integrals can be used. For the details of the solution we refer to references 6 and 7; here we only

give the final results.

In zeroth order with no collisions the distribution function $f^{(0)}$ has the following form:

$$f^{(0)}(\underline{r},\underline{k}) = f_o(\varepsilon_k + \phi(\underline{r}) - \phi(s = -\infty)) \ . \tag{8}$$

The potential $\phi(s = -\infty)$ depends on the beginning of the trajectory of an electron according to $\phi(z = \pm\infty) = \pm eV/2$ and causes a strong anisotropy in the kinetic energy distribution of the electrons near the contact area. For a spherical Fermi surface we have drawn schematically in Figure 2a the deformed Fermi surfaces at positions on both sides of the orifice. Charge neutrality gives in zeroth order the potential

$$\phi^{(0)}(\underline{r}) = \pm \frac{eV}{2}\left(1 - \frac{\gamma(\underline{r})}{2\pi}\right) , \tag{9}$$

where $\gamma(\underline{r})$ is the solid angle under which the orifice can be seen at a position $\underline{r}$. The $\pm$ sign refers to both sides of the contact. Using the zeroth order distribution function for the electrons as depicted in Figure 2 the Sharvin current through a contact can be calculated with equation (4). The final result is the Sharvin resistance as given in equation (2).

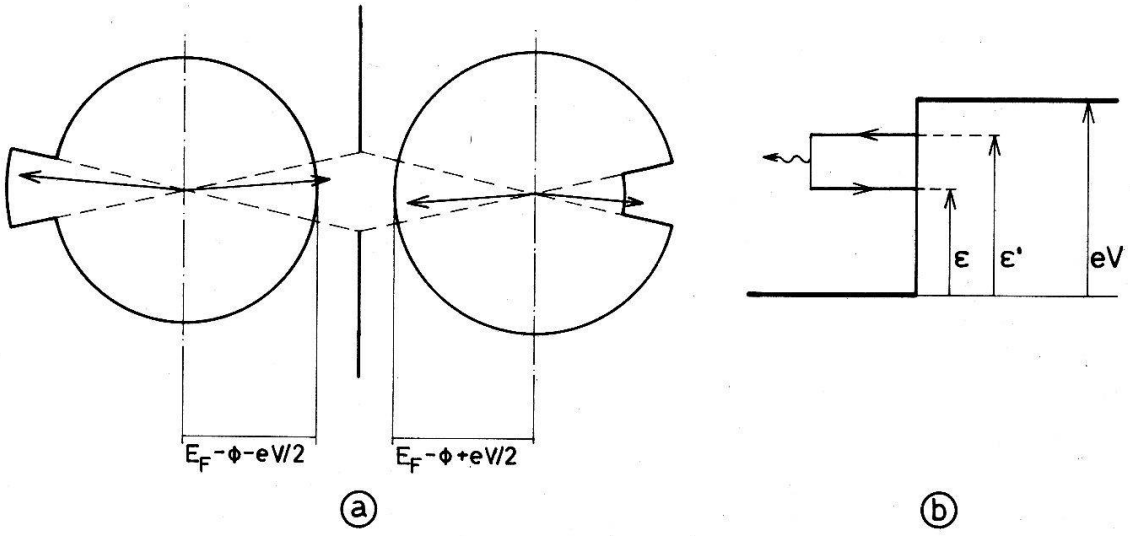

Figure 2. In part a the deformed Fermi spheres at two symmetrical points with respect to the contact which enter in the description of the transport problem. The arrows indicate inelastic collision processes for which the relevant energy levels are given in part b.

In next order the collision term has to be taken into account. Specifically, we consider the electron-phonon interaction, and then the collision term is given by

$$\left.\frac{\partial f(\underline{r},\underline{k})}{\partial t}\right|_{coll.} = \frac{2\pi}{\hbar}\sum_{\underline{k}'}|g_{kk'}|^2\{f(\underline{r},\underline{k}')[1-f(\underline{r},\underline{k})]\,\delta(\varepsilon_{k'}-\varepsilon_k-\hbar\omega) - f(\underline{r},\underline{k})[1-f(\underline{r},\underline{k}')]\,\delta(\varepsilon_k-\varepsilon_{k'}-\hbar\omega)\}\ . \qquad (10)$$

$g_{kk'}$ is the matrix element for the electron-phonon interaction. In the expression for the collisions we have ignored the distribution of phonons, because we are in the limit of low temperatures and consider only spontaneous emission of phonons. The first order contribution to $f(\underline{r},\underline{k})$ is a path integral

$$f^{(1)}(\underline{r},\underline{k}) = \int_{-\infty}^{o}\frac{ds}{|v_k|}\left.\frac{\partial f}{\partial t}\right|^{(0)}_{coll.}\ , \qquad (11)$$

which runs along a straight line starting far from the orifice ($s = -\infty$) and ending at the orifice ($s = 0$). Due to the specific shape of the Sharvin distribution $f^{(0)}$ the path integral contributes only within the common volume of two cylinders through the boundary of the orifice and with walls parallel to $\underline{k}$ and $\underline{k}'$. In the expression for the current the factor $\int d^2\underline{r}\int v_{\underline{k}z}\frac{ds}{|v_k|}$ just equals the common volume of these two cylinders. For the spontaneous emission of phonons the relevant energy levels are given schematically in Figure 2b. As a final result we get for the first-order correction to the current

$$I^{(1)} = -\frac{4\pi}{3}\frac{e}{\hbar}a^3N_o\int_o^{eV}d\varepsilon\int_{\varepsilon}^{eV}d\varepsilon'\ \alpha^2F_p(\varepsilon'-\varepsilon) \qquad (12)$$

for a circular orifice. N_o is the density of states for electrons at the Fermi level. The function α^2F_p for the electron-phonon interaction as detected by point contacts is given by

$$\alpha^2F_p = \frac{N_o}{32\pi^2}\int d^2\underline{n}\int d^2\underline{n}'\ |g_{nn'}|^2\ \eta(\theta_{nn'})\ . \qquad (13)$$

$\underline{n}$ and $\underline{n}'$ are the unit vectors parallel to $\underline{k}$ and $\underline{k}'$ and $\theta_{nn'}$ is the angle between these two vectors. The efficiency function for scattering of electrons with phonons using point contacts is

$$\eta(\theta) = \tfrac{1}{2}\ (1 - \theta/\mathrm{tg}\theta)\ . \qquad (14)$$

Note, that this formula diverges for 180^o back-scattering. The given formula for α^2F_p holds for isotropic scattering along the Fermi sphere. Kulik[6] has

given a more general expression for α^2F_p for the case where the scattering depends explicitly on the directions $\underline{n}$ and $\underline{n}'$. By a transformation both formula's reduce to identical ones[8]. In the transport problem for bulk material the well known efficiency function $(1 - \cos\theta)$ appears in the formula for α^2F. Twice differentiating equation (12) gives for the logarithmic derivative of the resistance

$$\frac{1}{R}\frac{dR}{dV} = - R_{Sh}\frac{d^2I}{dV^2} = \frac{16}{3}\frac{e}{\hbar v_F} a\, \alpha^2F_p(eV) \ . \qquad (15)$$

The contact radius a can be obtained from the Sharvin resistance.

So far we have applied the solution of the Boltzmann equation to the collision of electrons with phonons. The point-contact theory can be extended to any arbitrary scatterer[9]. Realizing that the inverse scattering time for an electron with energy eV above the Fermi level can be written as

$$\frac{1}{\tau}(eV) = \frac{2\pi}{\hbar}\int_0^{eV} d\varepsilon\ \alpha^2F(\varepsilon) \qquad (16)$$

and using equation (12) the differential resistance increases upon applying a voltage as

$$\left(\frac{dV}{dI}\right)_V - \left(\frac{dV}{dI}\right)_0 = - R_{Sh}^2\frac{dI}{dV} = \frac{2}{3}e^2a^3R_{Sh}^2N_o\frac{1}{\tau}(eV) \ . \qquad (17)$$

This expression is the grand result of point-contact spectroscopy. The inverse scattering time of an electron with energy eV above the Fermi level can be measured directly.

Electron-phonon interaction: α^2F

The point-contact method has been applied most successfully to an experimental study of the electron-phonon interaction in metals. The first pioneering experiments were done by Yanson with shorted tunnel junctions of superconductors like Pb, In and Sn [1]. The measured point-contact spectra agreed very well with tunneling data of the function α^2F, which were extracted from the measured density of states of the electrons via the Rowell-McMillan scheme. After these very first experiments pressure-type contacts were used for the study of normal metals, where no experimental data for α^2F were available[2]. In Figure 3 we have plotted some spectra for the noble metals Cu, Ag and Au. The three phonon modes (two transverse and one longitudinal) are clearly visible in the spectra. In this figure, the dashed lines represent the phonon density of states for these metals as obtained from neutron-

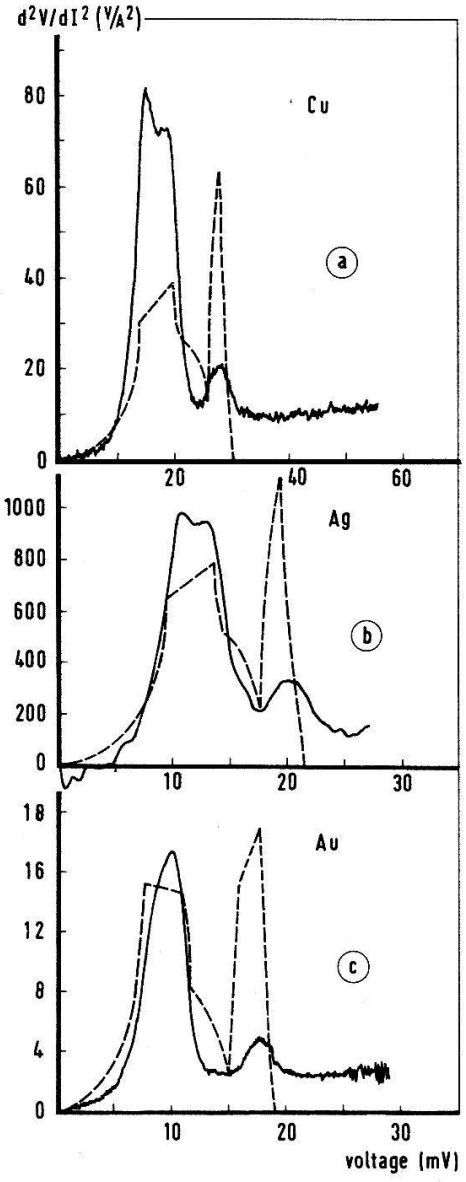

Figure 3. The d^2V/dI^2-curves of point contacts of the noble metals together with the phonon densities of states F from neutron experiments (broken curves). (a) R = 3.3 Ω, T = 1.5 K; (b) R = 16.3 Ω, T = 1.2 K; (c) R = 3.3 Ω, T = 1.2 K.

scattering experiments. By comparing the intensity of the point-contact spectra with neutron data it is seen that the longitudinal mode couples less with the electrons than the transverse modes. Band-structure calculations show that d-electrons are important in the noble metals and are strongly coupled with phonons via umklapp scattering. In a recent pseudo-potential calculation for Cu the importance of the efficiency function $\eta(\theta)$ has been demonstrated for the enhanced coupling with transverse phonons[10]. Similar coupling effects for the d-electrons with phonons were observed in the point-contact spectra of the real d-metals Fe, Co and Ni [11].

For the simple alkali-metals K, Na and Li detailed pseudo-potential calculations exist for the electron-phonon interaction. Therefore it was interesting to measure the spectra for these materials[12]. As an example we give in Figure 4 the measured phonon spectrum using a point contact with sodium. In the same figure the phonon density of states F has been included

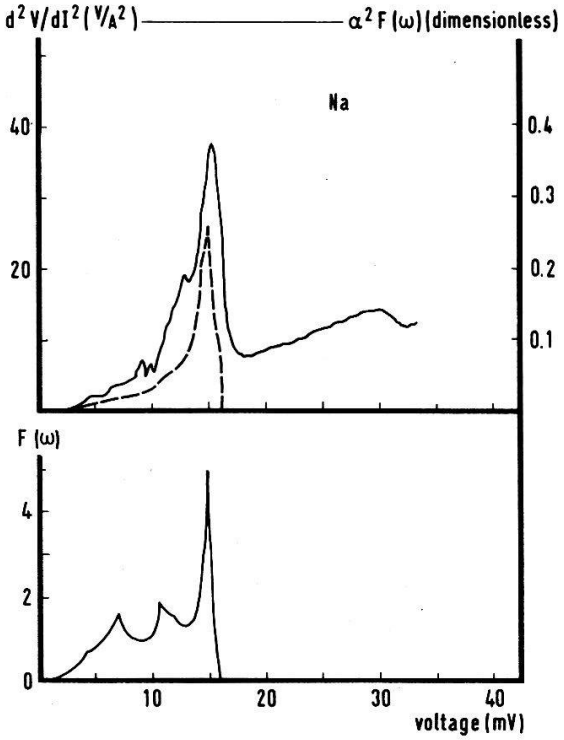

Figure 4. The d^2V/dI^2-curve for a point contact of sodium together with the phonon density of states F from neutron data and the α^2F-function (broken curve) from theoretical pseudo-potential calculations[14]. R = 1.1 Ω, T = 1.5 K.

obtained from neutron scattering and α^2F from theoretical calculations. The agreement is very good and confirms the pseudo-potential theory. In the spectrum for Na a structure is seen at higher voltages corresponding to twice the phonon frequencies. This observation is ascribed to double phonon processes[13]. The electrons are scattered back after the emission of two phonons, which yields the structure at double frequencies.

Using equation (15) the experimental data can be converted in absolute values for the electron-phonon interaction α^2F_p. The mass-enhancement factor $\lambda = 2 \int (\alpha^2F/\omega)d\omega$ can now be calculated, which gives the renormalization of the electron mass at the Fermi surface due to the coupling with phonons via $m^* = m(1 + \lambda)$. In this way reasonable values for λ have been determined for metals investigated with point contacts. For an exact evaluation of α^2F_p we have to realize that the measured spectra should be zero above the Debye energy. In the spectra a "background"-signal is observed. The explanation of the background is based on the assumption that the phonon system is not in thermal equilibrium. Phonons are spontaneously emitted at the contact region. These generated phonons lead to stimulated emission and absorption of phonons by the electrons and the additional backflow of electrons gives an extra

increase in resistance. According to a theoretical analysis of this phenomenon[5] the background signal saturates above the Debye energy as observed for spectra with relative small background signals (see Figure 3). Reference 7 gives a survey of the methods which have been used to correct the measured spectra for the background.

Other scattering mechanisms

Besides phonons also other scatterers for the electrons have been detected with point-contact spectroscopy. In point contacts with Gd, Ho and Tb singularities have been observed in the d^2V/dI^2-spectra at voltages corresponding to the magnons in these metals[15]. Thus the energy dependence of the electron-magnon coupling can be studied experimentally. We already mentioned the measurement of the phonon spectra in point contacts of the ferromagnets Fe, Co and Ni [11]. Beside these effects strong non-linearities were found at much higher voltages (200 - 300 mV), which were interpreted in terms of a heating model. At these high voltages the metal is heated up above the Curie temperature at the contact area and an increase in contact resistance is observed due to an increase in resistivity at the ferromagnetic transition-point. For two classes of compounds with intermediate valencies point-contact studies have been done. In the intermediate-valence compounds SmB_6 and TmSe sharp maxima have been observed in the resistance at zero voltage and explained with a hybridization gap in these materials[16]. The interpretation is analogous to the maxima in the resistance of superconducting point contacts due to the energy gap of the superconductor. The other type of mixed-valent samples has no semiconducting but metallic behaviour in the resistivity as a function of temperature. The resistance of a point contact for these materials (YbCuAl, $YbCu_2Si_2$) is minimal at zero bias-voltage and increases at typical excitation energies for the interaction of electrons with mixed valencies[17].

The specific scattering of electrons with paramagnetic impurities has been observed in point contacts with magnetically dilute alloys (Kondo systems, spin glasses)[9]. In the following we present point-contact experiments of the host-metal Au with small concentrations Mn (0.03, 0.1 and 0.3 at %)[18], where both parts of the contact were made from the same starting material. For the sample with the lowest impurity concentration the measured differential resistance of a contact has been plotted as a function of voltage in Figure 5. At low bias voltages a maximum in the resistance can be seen and above 4 mV the resistance increases again due to the electron-phonon coupling. The energy

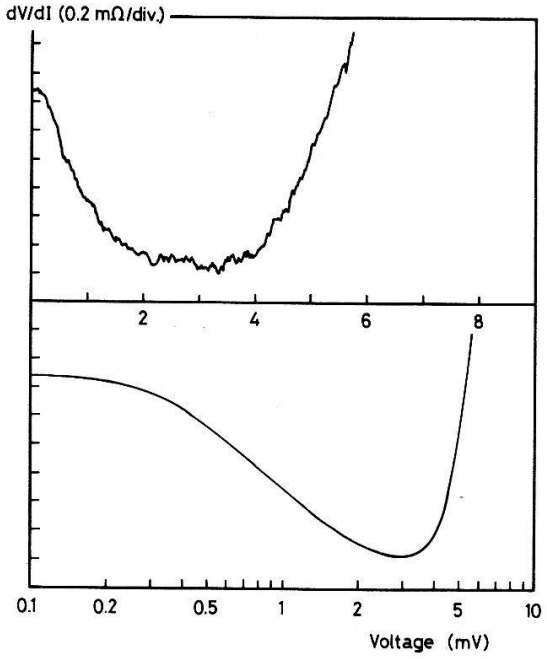

Figure 5. Differential resistance of a Au-0.03 at. % Mn point-contact as a function of the applied voltage (linear and logarithmic scale), which shows the Kondo anomaly at low bias voltages. R = 0.6 Ω; T = 1.2 K.

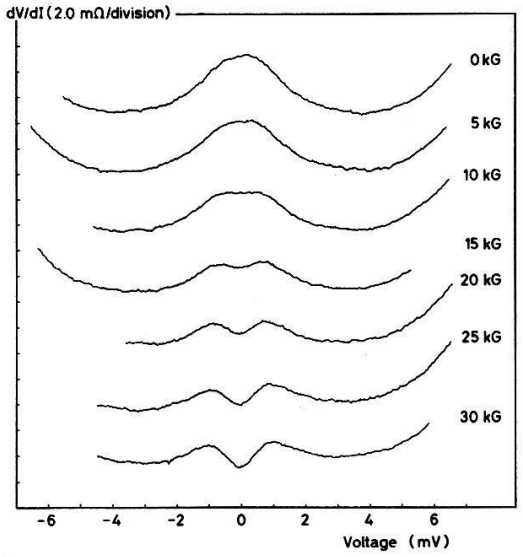

Figure 6. Magnetic field dependence of the differential resistance of a Au-0.1 at. % Mn point-contact. The curves have been shifted with respect to each other. R = 2.5 Ω; T = 1.5 K.

dependence of the inverse scattering time $1/\tau$ has been calculated for the s-d exchange interaction between local and conduction electrons for a Kondo system[19] with reliable solutions for eV, $k_B T > k_B T_K$, where T_K is the characteristic Kondo temperature of the dilute alloy (T_K for AuMn $\sim$ 0.01 K). The result of these calculations is a logarithmic energy dependence of $1/\tau$, which yields the characteristic logarithmic temperature dependence of the bulk resistivity of Kondo systems. The change in the differential resistance of a point contact is a direct measure for the scattering rate. Therefore we have also plotted the data in Figure 5 on a logV-scale. Only over a limited range the voltage dependence is logarithmic. At the low voltage side the deviation is probably due to thermal smearing or ordering effects and at high voltages the phonon structure becomes important. In Figure 6 we have presented the magnetic field dependence of a AuMn-point contact. With an applied magnetic field H the maximum at zero voltage splits up. The spin-flip process of the conduction

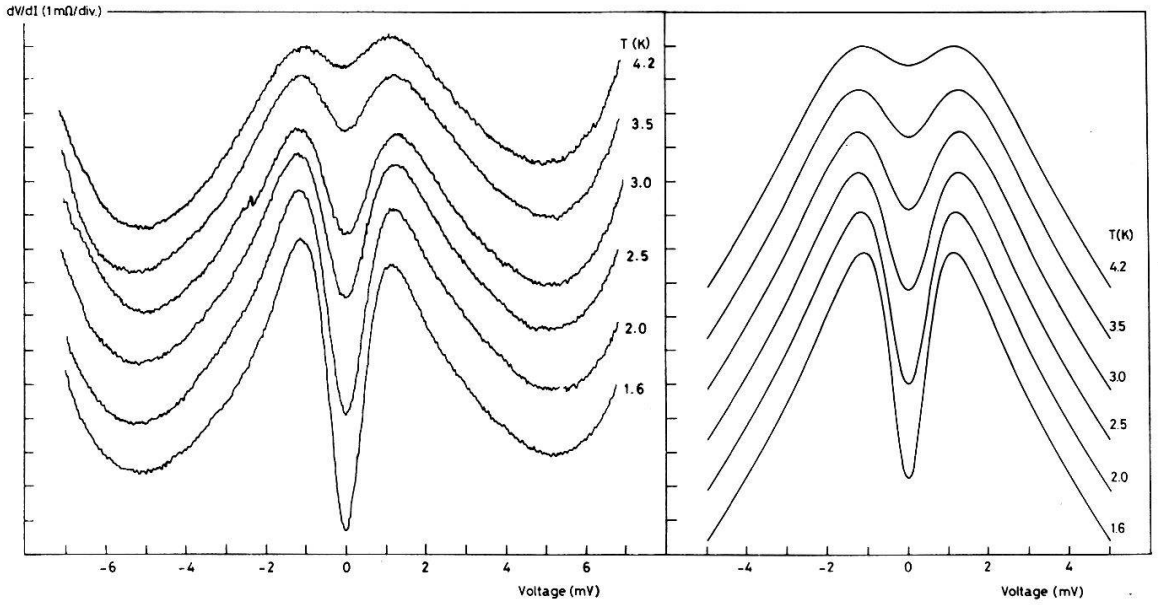

Figure 7. Experimental (left) and theoretical (right) curves for the differential resistance of a Au-0.3 at.% Mn point-contact at different temperatures. The curves have been shifted with respect to each other. R = 1.5 Ω.

electrons by the localized electrons costs an energy $\Delta = g\mu_B H$ and the Kondo anomaly at zero bias will be suppressed. At applied voltages $V = \pm g\mu_B H/e$ the point-contact resistance reveals maxima analogous to the zero-field case, because now the accelerated electrons can supply an energy eV for a spin-flip process. Using the appropriate scattering term for the exchange interaction a theoretical calculation describes the experimental result rather well[20]. From the magnetic field dependence of the point-contact resistance g-values can be measured for the Kondo systems from the distance between the maxima $2\Delta = 2g\mu_B H$. Upon increasing the concentration of magnetic impurities the interactions between the local moments become important and the samples enter the spin-glass regime. In Figure 7 the resistance of a Au-0.3 at.% Mn point-contact has been plotted for various temperatures below 4.2 K. Already at zero magnetic field the resistance is split up into two peaks with respect to V = 0. The indirect exchange interaction (RKKY) between the impurities yields an internal field H_{int}. The distance between the maxima $2\Delta = 2g\mu_B H_{int}$ reflects the distribution of internal fields. The temperature dependence is due to the competition between spin ordering in a magnetic field and thermal spin fluctuations. At the right-hand side of Figure 7 we have presented the calculated

spectra. To take account in these calculations for the RKKY-interaction between local moments a distribution of internal fields was used as described in reference 21 and a weighted average was performed for the spectra according to this internal field distribution. In a computer simulation of a spin-glas system[21] it was predicted that the internal field should increase below the spin-glass transition-temperature, where the impurity spins are strongly correlated. From our experiment shown in Figure 7 we conclude that the internal field stays constant for this particular sample in the investigated temperature range. It is interesting to study the internal fields using point contacts for an experimental verification of the computer-model.

This work is part of the research program of the Stichting voor Fundamenteel Onderzoek der Materie (Foundation for Fundamental Research on Matter) and was made possible by financial support from the Nederlandse Organisatie voor Zuiver-Wetenschappelijk Onderzoek (Netherlands Organization for the Advancement of Pure Research).

*Max-Planck-Institut für Festkörperforschung, Heisenbergstrasse 1, 7 Stuttgart 80, Federal Republic of Germany.

References

1. I.K. Yanson, Zh. Eksp. Teor. Fiz. 66, 1035 (1974) [Sov. Phys. - JETP 39, 506 (1974)].
2. A.G.M. Jansen, F.M. Mueller and P. Wyder, Phys. Rev. B 16, 1325 (1977).
3. J.C. Maxwell, A. Treatise on Electricity and Magnetism (Clarendon, Oxford, 1904).
4. Yu.V. Sharvin, Zh. Eksp. Teor. Fiz. 48, 984 (1965) [Sov. Phys. - JETP 21, 655 (1965)].
5. A.P. van Gelder, Solid State Commun. 25, 1097 (1978) and Solid State Commun. 35, 19 (1980).
6. I.O. Kulik, A.N. Omel'yanchuk and R.I. Shekhter, Fiz. Nizk. Temp. 3, 1543 (1977) [Sov. J. Low Temp. Phys. 3, 740 (1977)].
7. A.G.M. Jansen, A.P. van Gelder and P. Wyder, J. Phys. C: Solid State Phys. 13, 6073 (1980).
8. A.P. van Gelder, A.G.M. Jansen and P. Wyder, Physica 109-110B, 1955 (1982).
9. A.G.M. Jansen, A.P. van Gelder, P. Wyder and S. Strässler, J. Phys. F: Metal Phys. 11, L15 (1981).
10. M.J.G. Lee, J. Caro, D.G. de Groot and R. Griessen, to be published.

11. B.I. Verkin, I.K. Yanson, I.O. Kulik, O.I. Shklyarevski, A.A. Lysykh and Yu.G. Naydyuk, Solid State Commun. 30, 215 (1979).
12. A.G.M. Jansen, J.H. van den Bosch, H. van Kempen, J.H.J.M. Ribot, P.H.H. Smeets and P. Wyder, J. Phys. F: Metal Phys. 10, 265 (1980).
13. A.P. van Gelder, A.G.M. Jansen, S. Strässler and P. Wyder, J. Phys. (Paris) 39, C6-602 (1978).
14. J.P. Carbotte and R.C. Dynes, Phys. Rev. 172, 476 (1968).
15. A.I. Akimenko and I.K. Yanson, Pis'ma Zh. Eksp. Teor. 31, 209 (1980) [JETP Lett. 31, 191 (1980)].
16. I. Frankowski and P. Wachter, Solid State Commun. 41, 577 (1982).
17. B. Bussian, I. Frankowski and D. Wohlleben, Phys. Rev. Lett. 49, 1026 (1982).
18. The samples were prepared by Dr. B. Knook at the Kamerlingh Onnes Laboratorium and are registered under KOL 78135-137.
19. H. Suhl, ed. Magnetism vol. V (New York, Academic Press, 1973).
20. N. d'Ambrumenil and R.M. White, J. Appl. Phys. 53, 2052 (1982).
21. L.R. Wachter and R.E. Walstedt, Phys. Rev. B 22, 3816 (1980).